Influence of Membrane Surface Charge and Post-Translational Modifications to Myelin Basic Protein on Its Ability To Tether the Fyn-SH3 Domain to a Membrane in Vitro[†]

Lopamudra Homchaudhuri,[‡] Eugenia Polverini,[§] Wen Gao,[‡] George Harauz,[||] and Joan M. Boggs*[,‡]

Department of Molecular Structure and Function, Research Institute, Hospital for Sick Children, Toronto, Ontario, Canada M5G 1X8, Department of Laboratory Medicine and Pathobiology, University of Toronto, Toronto, Ontario, Canada M5G 1L5, Dipartimento di Fisica and CNISM, Universitá di Parma, V. le Usberti, 7/A, 43100 Parma, Italy, and Department of Molecular and Cellular Biology and Biophysics Interdepartmental Group, University of Guelph, Guelph, Ontario, Canada N1G 2W1

Received December 11, 2008; Revised Manuscript Received January 27, 2009

ABSTRACT: Myelin basic protein (MBP) is a highly post-translationally modified, multifunctional structural component of central nervous system myelin, adhering to phospholipid membranes and assembling cytoskeletal proteins, and has previously been shown to bind SH3 domains in vitro and tether them to a membrane surface [Polverini, E., et al. (2008) *Biochemistry 47*, 267−282]. Since molecular modeling shows that the Fyn-SH3 domain has a negative surface charge density even after binding the MBP ligand, we have investigated the influence of negative membrane surface charge and the effects of post-translational modifications to MBP on the interaction of the Fyn-SH3 domain with membrane-associated MBP. Using a sedimentation assay with multilamellar vesicles consisting of neutral phosphatidylcholine (PC) and negatively charged phosphatidylinositol (PI), we demonstrate that increasing the negative surface charge of the membrane by increasing the proportion of PI reduces the amount of Fyn-SH3 domain that binds to membrane-associated MBP, due to electrostatic repulsion. When one of the phosphoinositides, PI(4)P or PI(4,5)P_2 was substituted for PI in equal proportion, none of the Fyn-SH3 domain bound to MBP under the conditions that were used. Post-translational modifications of MBP which reduced its net positive charge, i.e., phosphorylation or arginine deimination, increased the degree of repulsion of Fyn-SH3 from the membrane surface, an effect further modulated by the lipid charge. This study suggests that changes in membrane negative surface charge due to protein or lipid modifications, which could occur during cell signaling, can regulate the binding of the Fyn-SH3 domain to membrane-associated MBP and thus could regulate the activity of Fyn at the oligodendrocyte membrane surface.

Myelin basic protein (MBP)[1] is the second most abundant protein, 30% of the total protein by weight, in central nervous system (CNS) myelin, after proteolipid protein (*1*). MBP has a high net positive charge (pI ∼10) and binds to the polar headgroups of acidic lipids via electrostatic interactions at the cytoplasmic leaflet of oligodendrocytes (*2*−*5*). Its principal role is in adhesion of the cytosolic surfaces of the multilayered compact myelin sheath, whose structural integrity determines the speed of transmission of action potentials along the axon. However, MBP seems to be a multifunctional protein, since it also interacts with other proteins such as the cytoskeletal proteins actin, tubulin, and Ca^{2+}-calmodulin and causes polymerization and bundling of actin and tubulin (*2, 6*−*9*). Through its highly conserved proline-rich region, TPRTPPP, corresponding to residues T92−P98, murine sequence numbering (T94−P100, bovine sequence numbering), it was predicted to be a ligand for SH3 domains (*10*) and recently shown to bind SH3 domains from several different proteins, including the Src tyrosine kinase Fyn (*11*).

We further showed that MBP can bind the Fyn-SH3 domain (Fyn-SH3) to a membrane surface (*11*), as shown earlier for actin filaments (*7*). Thus, MBP may tether cytoskeletal and signaling proteins to the oligodendrocyte or myelin plasma membrane as a membrane scaffolding protein. Compartmentalization of signaling molecules by binding to membrane domains and scaffolding proteins is an important means of regulating their activity and achieving

[†] This work has been supported primarily by the Multiple Sclerosis Society of Canada (Operating Grant to J.M.B.) and the Natural Sciences and Engineering Research Council of Canada (NSERC, Discovery Grant RG121541 to G.H.). L.H. was the recipient of a postdoctoral fellowship from the Multiple Sclerosis Society of Canada.

* To whom correspondence should be addressed: Department of Molecular Structure and Function, Research Institute, Hospital for Sick Children, 555 University Ave., Toronto, Ontario, Canada M5G 1X8. Phone: (416) 813-5919. Fax: (416) 813-5022. E-mail: jmboggs@sickkids.ca.

[‡] Hospital for Sick Children and University of Toronto.

[§] Universitá di Parma.

[||] University of Guelph.

[1] Abbreviations: bC1, bovine myelin basic protein, C1 component; Fyn-SH3, recombinant SH3 domain of chicken Fyn; MAPK, mitogen-activated protein kinase; MARCKS, myristoylated alanine-rich C kinase substrate; MBP, myelin basic protein; MLV, multilamellar vesicles; OL, oligodendrocyte; Ph-bC1, phosphorylated bovine myelin basic protein C1 component; rmC1, recombinant murine myelin basic protein C1 component; rmC8, recombinant murine myelin basic protein C8 component; PC, phosphatidylcholine; PDB, Protein Data Bank; PI, phosphatidylinositol; PIP, phosphatidylinositol 4-monophosphate; PIP_2, phosphatidylinositol 4,5-bisphosphate.

10.1021/bi8022587 CCC: $40.75
Published on Web 01/29/2009

specificity of their effects in cells (*12, 13*). To determine mechanisms of regulation of the ability of MBP to tether proteins to the membrane, in this paper, we investigate the influence of negative membrane surface charge on the interaction of Fyn-SH3 with membrane-associated MBP.

Fyn-SH3 is made up of 60 amino acid residues corresponding to T82−S143, human sequence numbering. Previously, molecular modeling showed that basic residues in the MBP SH3 ligand domain, residues T92−R104 (murine sequence numbering), canonically interact via salt bridges and cation−π interactions with several acidic and aromatic residues in the SH3 domain binding site (*11*). However, the SH3 domain has an excess of acidic residues around the hydrophobic ligand binding site. A basic protein bound to a lipid bilayer can create a positive electrostatic potential above the membrane surface, as demonstrated for the MARCKS (myristoylated alanine-rich C kinase substrate) effector domain (*14*). However, as the amount of negatively charged lipid increases or the net positive charge of the basic protein decreases, the surface potential of the membrane in the vicinity of the protein will become negative, causing repulsion of a tethered negatively charged protein, as shown for actin filaments (*7*). Negative charges may be generated on a membrane cytoplasmic surface during signal transduction processes by phosphorylation of inositol lipids, by the generation of phosphatidic acid, or by the release of acidic lipids from protein-bound complexes, as in the case of phosphatidylinositol 4,5-bisphosphate (PIP_2) (*15*−*19*). Post-translational modifications of MBP, phosphorylation and deimination, can cause release of PIP_2 from MBP (*18*) and also increase the negative surface charge of the membrane (*20*).

MBP undergoes extensive post-translational modifications, e.g., phosphorylation, deamidation, and deimination of six Arg residues to citrulline, which modify the net charge of the protein (*21, 22*). The least modified form isolated from myelin MBP is called C1, and the deiminated form is called C8. Phosphorylation and deimination occur during both myelin development and function, and deimination may be involved in the pathogenesis of multiple sclerosis (*2, 6, 22*−*25*). The TPRTP sequence of MBP carries two threonine residues, T94 and T97, bovine sequence numbering (T92 and T95, murine sequence numbering), which are mitogen-activated protein kinase (MAPK) targets (*26, 27*). These post-translational modifications of MBP affect its targeting to microdomains in myelin in vivo (*28, 29*) and modulate its interactions with lipid membranes (*20, 21, 30, 31*) and with proteins such as calmodulin, actin, and tubulin (*2, 6, 8, 9, 23, 32*−*34*). These modifications to membrane-associated MBP would increase the negative charge of the membrane surface. In this study, we determine the effect of membrane surface charge on the ability of MBP to tether Fyn-SH3 to a lipid membrane by varying the ratio of phosphatidylinositol (PI) to phosphatidylcholine (PC), by substituting more highly phosphorylated forms, phosphatidylinositol 4-monophosphate (PIP) and PIP_2 for PI, and by MAPK phosphorylation and pseudodeimination of MBP.

MATERIALS AND METHODS

The least modified, most highly positively charged 18.5 kDa component of MBP, bC1, purified from bovine brain MBP (*35*) was used. The recombinant murine, pseudodeiminated C8 component, in which Gln is substituted for six citrullines, rmC8, was generated from recombinant murine 18.5 kDa MBP by sequential site-directed mutations (first R25Q, and then R33Q, K119Q, R127Q, R157Q, and finally R168Q, murine sequence numbering) via the QuikChange protocol (Stratagene, La Jolla, CA), as described previously (*36*). The protein bC1 was phosphorylated by p42 MAPK (New England Biolabs) at Thr94 and Thr97 (bovine sequence) to yield phosphorylated bovine C1 (Ph-bC1) (*34*). Electrophoresis on alkaline tube gels revealed that most of the bC1 was doubly phosphorylated (*11*). The SH3 domain of Fyn, residues 85−142, containing a FLAG epitope and a His_6 tag at the C-terminus, and a short N-terminal tail, was a kind gift from A. Davidson (University of Toronto) and was prepared and purified as described previously (*37*).

Egg L-α-phosphatidylcholine (PC), L-α-phosphatidylinositol (PI, sodium salt, from bovine liver), L-α-phosphatidylinositol 4-monophosphate (PIP) (ammonium salt, from porcine brain), and L-α-phosphatidylinositol 4,5-bisphosphate (PIP_2) (ammonium salt, from porcine brain) were purchased from Avanti Polar Lipids, Inc. (Alabaster, AL). The [^{3}H]cholesterol (specific activity of 5 mCi/μmol) was from Amersham (Baie d'Urfe, QC).

Mouse anti-Fyn antibody was purchased from Thermo Scientific (Fremont, CA); rat anti-MBP antibody was from abD Serotec (Oxford, U.K.), and donkey Cy2-conjugated anti-mouse IgG and donkey Cy3-conjugated anti-rat IgG were purchased from Jackson ImmunoResearch Laboratories Inc. (West Grove, PA).

Oligodendrocyte Cell Culture. Spinal cord oligodendrocytes from Wistar rat pups (7−8 days old; Charles River Canada, Saint-Constant, QC) were cultured as described previously (*38*). Cells were seeded at a concentration of 10^6 cells/mL on polylysine-coated coverslips and grown for 8−9 days.

Immunofluorescent Staining and Confocal Microscopy of Cultured Oligodendrocytes. Cells were fixed with 4% paraformaldehyde for 15 min at room temperature, washed four times with PBS (phosphate-buffered saline), permeabilized (0.05% saponin), and blocked with 5% normal goat serum and 5% normal donkey serum. Cells were then doubly immunostained for MBP and Fyn, using anti-MBP (1:800) and anti-Fyn (1:100) antibodies, respectively, in blocking solution. After extensive washing, appropriate dye-conjugated anti-IgG antibodies were incubated (2 h, gentle shaking) with the cells, followed by further washing. Coverslips were then mounted with IMMU-MOUNT medium (Thermo-Electron Corp., Pittsburgh, PA) and allowed to harden overnight, in the dark, on a flat surface. Slides were viewed in a Zeiss model LSM-510 confocal laser-scanning microscope controlled by the LSM-510 program and imaged using the sequential scanning mode.

Preparation of Multilamellar Vesicles. PC/PI, PC/PIP, and PC/PIP_2 MLV were prepared in mole ratios varying from 95:5 to 85:15. In each case, aliquots of PC and inositide lipids (PI, PIP, and PIP_2) were mixed together in chloroform. The [^{3}H]cholesterol was added to give a specific activity of approximately 200000 dpm/10 μmol of lipid, and the solvent was rapidly evaporated in a stream of nitrogen at 37 °C (*39*) to yield a lipid film containing 1 mg (1.3 μmol) of lipid. The resulting lipid film was then lyophilized overnight and

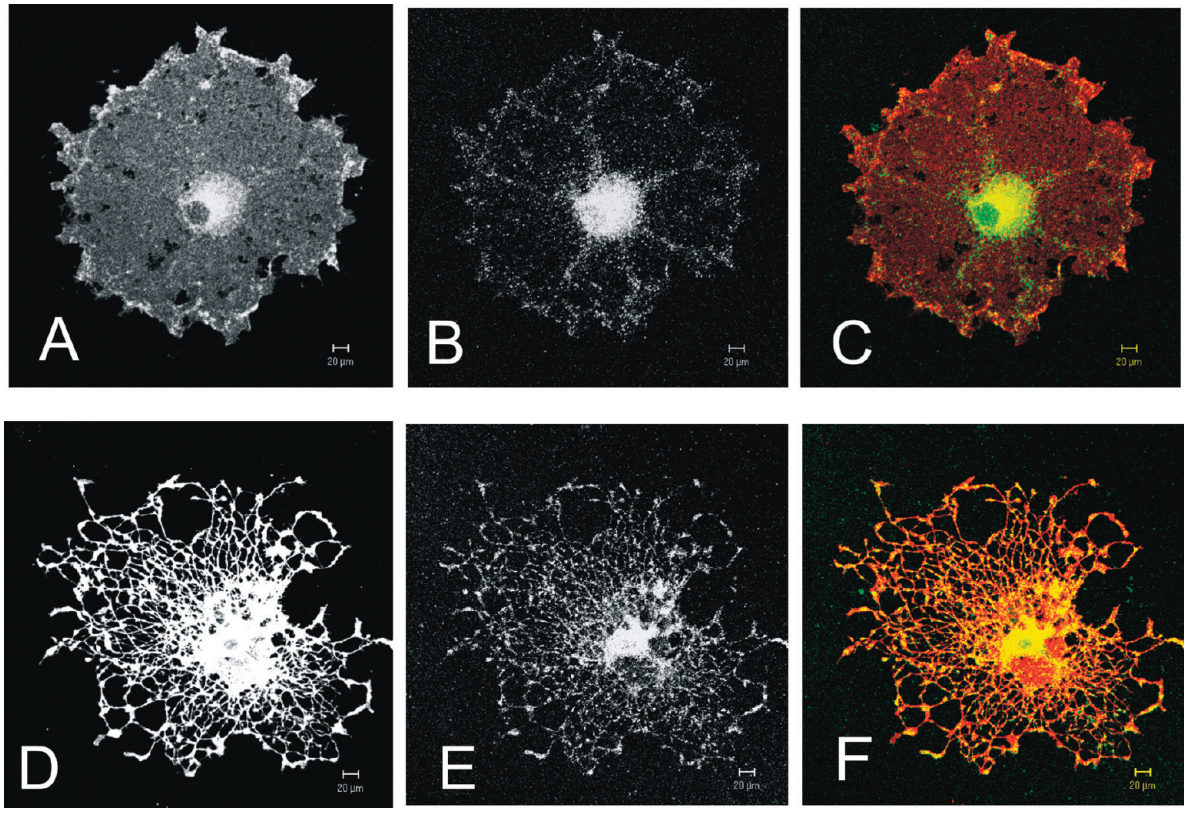

FIGURE 1: Confocal microscope images of cultured oligodendrocytes fixed, permeabilized, and costained with rat anti-MBP Ab and Cy3-conjugated anti-rat IgG (A and D) and mouse anti-Fyn and Cy2-conjugated anti-mouse IgG (B and E). Panel C is the merged image of panels A and B, and panel F is the merged image of panels D and E. MBP is colored red and Fyn green in panels C and F. A more mature cell with large membrane sheets is shown in panels A−C, and a less mature cell from the same culture with numerous membrane processes is shown in panels D−F. Colocalization of MBP and Fyn is seen at the edges of the membrane sheets as well as on major cytoskeletal veins in panels A−C and on the narrow membrane processes in panels D−F. The scale bar is 20 μm in each case.

vortexed vigorously in a 200 μL aliquot of 10 mM HEPES buffer containing 10 mM NaCl and 1 mM EDTA, adjusted to pH 7.4 with NaOH, to yield MLV. In experiments to determine the effect of ionic strength, MLV were also prepared in the same buffer containing 100 mM NaCl. The total Na^+ concentration was determined by flame photometry using an IL943 flame photometer and found to be 17 and 113 mM in the buffers containing 10 and 100 mM NaCl, respectively.

Interaction of Fyn-SH3 with Membrane-Associated MBP Components. MBP components bC1, Ph-bC1, and rmC8 were each dissolved in distilled water at concentrations of 3.2, 4.45, and 0.62 mg/mL, respectively, and the Fyn-SH3 domain was used as supplied in a 50 mM phosphate buffer containing 100 mM NaCl (pH 7.0), at a concentration of 1.74 mg/mL.

An aliquot containing 50 μg of each MBP component (2.8 nmol) and enough buffer [10 mM HEPES-NaOH (pH 7.4) containing 10 mM NaCl and 1 mM EDTA, unless otherwise noted] to attain a total volume of 390 μL was then added to 100 μL of MLV (0.65 μmol of lipid), mixed gently, and incubated at room temperature for 30 min. The MBP/MLV suspension was then treated with 10 μL containing 18.2 μg (2.8 nmol) of Fyn-SH3, mixed gently, and incubated at room temperature for 1 h. The mole ratio of each MBP component added to Fyn-SH3 was 1:1 in all cases. The final volume of the mixture was 500 μL.

The suspension was then centrifuged at room temperature at 16249*g* for 15 min in an Eppendorf bench centrifuge. The supernatant was removed, and the pellet was resuspended in pH 7.4 HEPES-NaOH buffer. Aliquots of the supernatant and pellet were then taken for counting of [^{3}H]cholesterol, for protein assay by the Peterson method (*40*), and for gel electrophoresis on 10% Bis-Tris NuPage gels (Invitrogen, Mississauga, ON) along with standards of bC1, Fyn-SH3, Ph-bC1, and rmC8. Coomassie blue-stained gels were analyzed with a UVP image analyzer (UVP, Upland, CA), and band densities were compared to those of the standards to quantify the amount of protein in each sample. Band densities were within the linear range.

Electrostatic Potential Analysis. The electrostatic potential surfaces were calculated by means of the tools available in version 4.0.1 of Swiss PdbViewer (*41*), using the Poisson−Boltzmann method, with atomic partial charges assigned following the Gromos96 force field parameter set (*42*), at pH 7 (histidines in the neutral form). The phosphate group was assumed, at the experimental pH, to have a net charge of −2; therefore, its partial charges were reassigned according to the method of Kollmann (*43*). The dielectric constant of the solvent was set to 80, and that of the interior of the protein was set to 4. The equipotential contours have cutoffs of −2 k_bT/e for the negative value and of 2 k_bT/e for the positive one (with the exception of Figure 2A; see the figure legend), represented by colors that go from red, through white (corresponding to 0 k_bT/e), to blue, respectively. The potential was mapped to the solvent accessible surface, calculated with a rolling probe of radius 1.4 Å. On the surface, the red to blue colors correspond to potential values ranging from −3 to 3 k_bT/e.

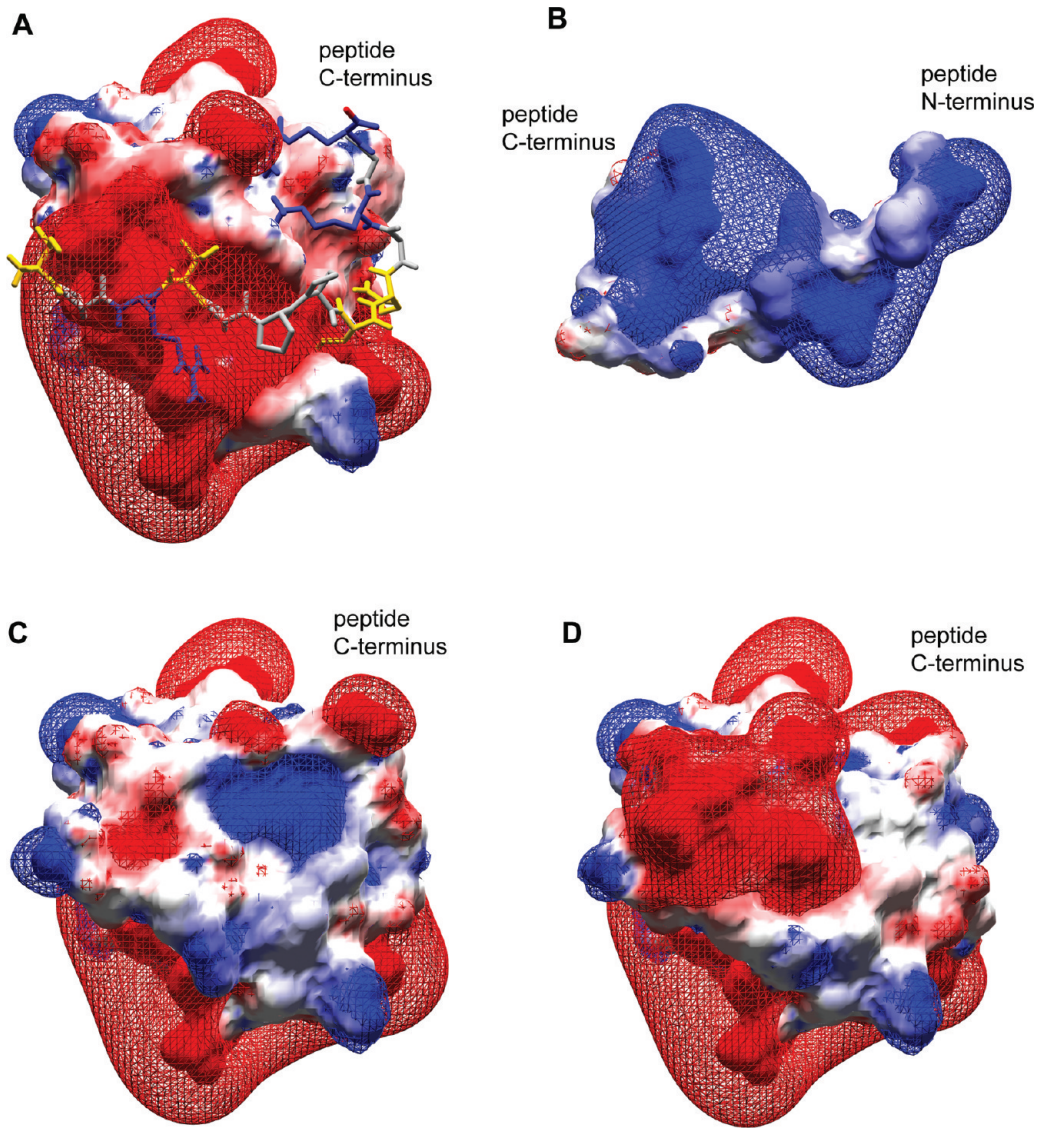

FIGURE 2: (A) Electrostatic potential surface calculated for the Fyn-SH3 domain alone, with the MBP T92−R104 peptide (murine sequence numbering) visualized in the position that it should have in the complex, based on molecular modeling (*11*). The electrostatic potential surface mesh wraps around the MBP peptide, which is in a stick representation, colored by amino acid type (polar ones are yellow, hydrophobic ones white, and positively charged ones blue). (B) Electrostatic potential surface of the MBP T92−R104 peptide (murine sequence numbering). The conformation of the peptide is taken from ref *11* and is oriented to show the surface that interacts with the SH3 domain. (C) Electrostatic potential surface of Fyn-SH3 complexed with the MBP T92−R104 peptide. Fyn-SH3 in the complex is oriented in exactly the same way as in panel A; the MBP peptide is facing in the opposite direction as in panel B. (D) Electrostatic potential surface of the Fyn-SH3 domain complexed with the MBP T92−R104 peptide phosphorylated on T92 and T95. The complex is oriented as in panel C. For the electrostatic potential surfaces, cutoffs of −2.5 k_bT/e for the negative value, in red, and of 2.5 k_bT/e for the positive one, in blue, were used for panel A, and cutoffs of −2 and 2 k_bT/e were used for panels B−D. Beneath the electrostatic potential surface (shown in a mesh representation), the peptide and the protein domain are visualized with their solvent-accessible surfaces, onto which the electrostatic potential is mapped.

A working model of the entire human Fyn kinase was built by superimposing the X-ray crystal structures of the SH3-SH2 and kinase domains [Protein Data Bank (PDB) entries 1G83 and 2DQ7, respectively (*44*)] on the crystal structure of human Src kinase [PDB entry 2SRC (*45*)] to obtain the correct reciprocal orientation of the domains. The N- and C-terminal regions and the linker peptide are missing but are not important for our purpose here. The conformation of the MBP T92−R104 peptide (murine sequence numbering), complexed with the Fyn-SH3 domain, was as we published previously (*11*).

RESULTS AND DISCUSSION

We previously showed that MBP could mediate binding of Fyn-SH3 to a lipid bilayer (*11*), suggesting that MBP might be able to tether Fyn to the oligodendrocyte (OL) membrane surface. Here, we show that Fyn is partially colocalized with MBP in membrane sheets formed by a mature OL, especially on the edges of the membrane and on the major cytoskeletal veins (Figure 1A). It is also extensively colocalized with MBP in the numerous processes formed by a less mature OL, whose processes have not yet expanded to membrane sheets (Figure 1B).

The SH3 domains bind ligands with a relatively low affinity (*46*), allowing exchange with different signaling proteins and dynamic changes in localization in response to local requirements. Changes in membrane surface potential due to changes in lipid composition occur during cell signaling and could be one mechanism of regulating local-

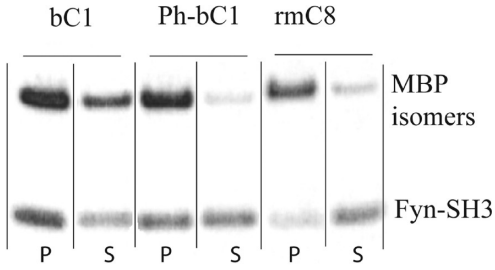

FIGURE 3: Polyacrylamide gel showing bands corresponding to MBP charge isomers and Fyn-SH3 obtained from lipid/protein mixtures that were centrifuged at 16249*g*. The resuspended pellets (P) (containing bound proteins) and the supernatants (S) (unbound proteins) were electrophoresed on an SDS gel. Each mixture contained PC/PI (90:10) lipid MLV and 1:1 mole ratios of one of the MBP charge isomers (bC1, Ph-bC1, and rmC8) and Fyn-SH3: lanes 1 and 2, bC1; lanes 3 and 4, Ph-bC1; and lanes 5 and 6, rmC8. The mole ratio of bound Fyn-SH3 to each MBP charge isomer was determined by comparing densities of the respective bands to protein standards bC1, Fyn-SH3, Ph-bC1, and rmC8 (1 μg of each) run on the same gel (not shown).

ization of soluble proteins tethered to the membrane by membrane proteins. Our previous molecular docking simulations estimated the dissociation constant of the Fyn-SH3 domain−MBP interaction to be on the order of micromolar (*11*). The Fyn-SH3 domain has a net negative charge that produces a large region of strong negative potential that surrounds and envelops the binding site (Figure 2A). The MBP peptide, T92−R104 (murine sequence numbering), whose interaction with Fyn-SH3 was modeled previously (*11*), has, on the other hand, a strong positive potential extending all around its surface (Figure 2B) that favors binding to Fyn-SH3. The resulting complex has an electrostatic equipotential surface less negative than Fyn-SH3 alone (Figure 2C) that could allow MBP to tether Fyn-SH3 to a lipid vesicle surface. As the negative charge on the membrane surface due to acidic lipids exceeds the positive charge contribution of MBP, the Fyn-SH3 domain might be repelled from it.

Here, we have investigated the influence of membrane negative surface charge on the ability of membrane-associated MBP to tether the Fyn-SH3 domain to the surface of lipid vesicles. Our assay uses MLV, which can be readily sedimented, to quantify protein bound to the membrane surface from a Coomassie-stained gel (Figure 3). Fyn-SH3 binds to the MLV only when MBP is also bound to them (*11*). The surface charge of the MLV has been modulated by varying the PC:PI mole ratio and by varying the phosphorylation of PI using one of the phosphoinositides (PI, PIP, or PIP_2) in a constant mole ratio to PC. We have also looked at the influence of post-translational modifications of MBP which reduce its net positive charge, phosphorylation by MAPK, and Arg deimination [using Gln as a mimic for citrulline in recombinant MBP (*36*)] on its ability to tether Fyn-SH3 to the membrane.

The Influence of the Membrane Negative Surface Charge Increased with an Increase in PI Content or by Phosphorylation of PI. The negative charge of the membrane surface was varied by increasing the amount of PI in the PC vesicles from 2.5 to 20 mol %. Figure 4 depicts the percentages of bC1 and Fyn-SH3 bound to the vesicles containing varying mole percentages of PI. Fyn-SH3 binds to the vesicles only if bC1 is bound (*11*). With an increasing mole percentage

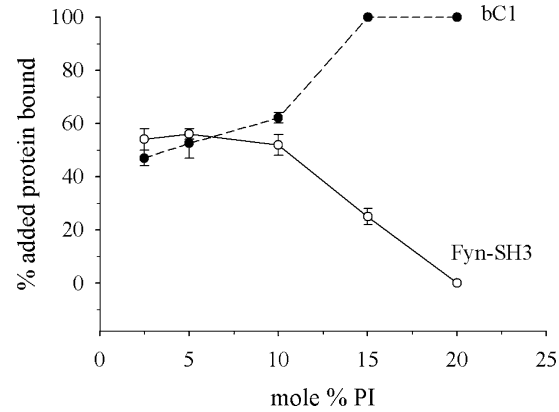

FIGURE 4: Increasing membrane surface charge weakens the binding of Fyn-SH3 to membrane-associated bC1. Negative surface charge was modulated by increasing the concentration of PI in PC/PI MLV from 2.5 to 20 mol %. The percentages of bound bC1 (●, dashed line) and Fyn-SH3 (○, solid line) are plotted vs PI concentration. Values represent means ± the range of two independent experiments except for the data point at 20 mol % which was included in only one of the experiments.

Table 1: Percentages of bC1 and Fyn-SH3 Bound to PC MLV Containing 5 mol % of One of the Phosphoinositides (PI, PIP, or PIP_2)

	% bound protein[a]	
inositide lipid	bC1	Fyn-SH3
PI	72.5 ± 6.1	69.7 ± 2.2
PIP	100	0
PIP_2	100	0

[a] Values represent the mean ± the range of two experiments.

of PI, more bC1 binds to the vesicles. However, despite this greater amount of ligand, the amount of bound Fyn-SH3 decreases with an increasing mole percentage of PI. This observation is a result of an increasing degree of electrostatic repulsion between the negatively charged membrane surface and Fyn-SH3, as the concentration of the acidic lipid PI in the PC/PI MLV is increased. Similar results were obtained using phosphatidylglycerol as the negatively charged phospholipid in the vesicles (not shown).

Roughly 70% of both the unmodified bC1 and Fyn-SH3 bound to the MLV containing 5 mol % PI and 95 mol % PC (Table 1). When either PIP or PIP_2 was substituted for PI in the vesicles, all of the added bC1, but none of the Fyn-SH3, bound to the lipid vesicles. PIP_2 is considered to have a valence of −4 in a lipid bilayer (*39*), in contrast to −1 for PI. The results observed may again be explained on the basis of electrostatic repulsion arising between PIP or PIP_2 and Fyn-SH3. The ability of MBP to cluster these lipids, particularly PIP_2 (*18*), will amplify the effect of the additional phosphate groups on PI.

Influence of Ionic Strength. The ionic strength was increased to determine if it could shield the negative charges of the vesicle surface and of Fyn-SH3 and thereby decrease their repulsion. In Figure 5, we show the effect of two different NaCl concentrations, 10 and 100 mM, on the mole ratio of Fyn-SH3 to bC1 bound to the lipid vesicles (the amount of bC1 bound did not change). The negative surface charge on the vesicles was varied using 2.5 to 20 mol % PI at 10 and 100 mM NaCl (see Figure 4). The amount of Fyn-SH3 bound to the vesicles decreased with an increase in negative surface charge in the presence of both 10 and 100 mM NaCl. However, the decrease in the level of binding is

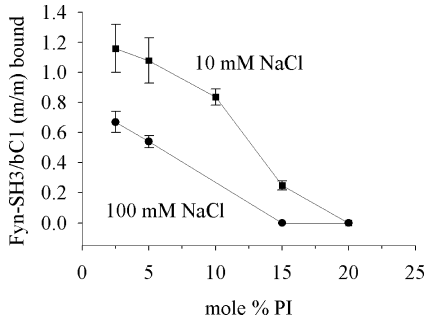

FIGURE 5: Influence of ionic strength on the interaction of Fyn-SH3 with membrane-associated MBP. The mole ratios of bound Fyn-SH3 to bC1 are plotted vs the concentration of PI in buffers at two NaCl concentrations, 10 (■) and 100 mM NaCl (●). The total Na^+ concentrations were 17 and 113 mM, respectively. Data represent the mean ± the range of two independent experiments using both NaCl concentrations.

even more drastic at higher ionic strengths, with complete dissociation of Fyn-SH3 from the vesicle surface at 15 mol % PI. This observation indicates that at higher ionic strengths, the salt bridges between charged residues of MBP and Fyn-SH3 are disrupted due to shielding of their charge, thus decreasing the affinity of the SH3 domain for MBP and overriding the effect of shielding the negative charge of the lipids.

In agreement with these hypotheses, the electrostatic equipotential surfaces, calculated at an ionic strength corresponding to a salt concentration of 100 mM, show that the overall magnitude of the electric field, surrounding both Fyn-SH3 and the MBP peptide, decreases in both its positive and negative values (Figure 6), thus reducing the affinity between the two molecules.

Influence of Post-Translational Modifications of MBP. The influence of post-translational modifications to MBP on the interaction between Fyn-SH3 and membrane-associated MBP at three different concentrations of PI, 7.5, 10, and 12.5 mol %, is shown in Figure 7. At 7.5 mol % PI, the three charge components of MBP (bC1, Ph-bC1, and rmC8) bind Fyn-SH3 to the same extent. However, at 10 mol % PI, the modified components, Ph-bC1 and rmC8, bound less Fyn-SH3 per mole of bound MBP to the vesicle surface than the most positively charged component, bC1. With a further increase in the negative surface charge of the vesicles, using 12.5 mol % PI, bC1 also bound less Fyn-SH3. Although post-translational modifications occurring in MBP in vivo decrease the affinity of MBP components for lipid bilayers (*31*), under the conditions used here, similar amounts of bC1, Ph-bC1, and rmC8 were bound to these vesicles (not shown). An increase in the negative charge on the membrane surface due to post-translational modifications of MBP thus also modulates the interactions between Fyn-SH3 and membrane-associated MBP components. These post-translational modifications of MBP increase the degree of repulsion of Fyn-SH3 from the membrane surface, and this effect is further modulated by the lipid charge.

If we analyze the electrostatic potential surface of the Fyn-SH3−MBP complex in which MBP is doubly phosphorylated (structure from ref *11*) (Figure 2D), we can observe the increase in the negative potential in the phosphate region, which could decrease the positive contribution of the electrostatic potential of whole MBP, thus decreasing the SH3 binding affinity and increasing the degree of repulsion between Fyn-SH3 and the negatively charged lipids at the membrane surface. Phosphorylation of MBP might also decrease the affinity of this domain for the lipid surface, but the remaining positively charged domains of MBP keep the MBP molecule bound to the lipid surface under these conditions.

Our observation of the effect of phosphorylation on membrane-associated MBP−Fyn-SH3 binding is related to a report by Reynolds et al. (*47*) on tau, which contains several PXXP motifs near Ser/Thr phosphorylation sites. Phosphorylation at these sites in vitro or in transfected cells reduced the level of binding of tau to SH3 domains from Fyn, p85α, PLCγ1, and the N-terminal SH3 domain of Grb2. Like MBP, tau also binds to membranes (*48, 49*), and both tau and Fyn are associated with rafts in OLs (*50*) as is MBP (*28, 51*). However, the ability of tau to bind SH3 domains to membranes and the effect of phosphorylation on that ability have not been investigated. Interestingly, the Pro-rich region of MBP also binds to the WW domain of the prolyl isomerases, human PIN-1 and yeast ESS1, when MBP is Thr-phosphorylated but not when it is unphosphorylated (*52*), as also found for tau (*47*), in agreement with the highly positive electrostatic potential surface of the WW domain (not shown). Thus, as for tau, the proline-rich region of membrane-associated MBP may bind one protein when phosphorylated and another protein when not phosphorylated.

CONCLUSIONS

Compartmentalization of signaling molecules by binding to membrane domains and scaffolding proteins is an important means of regulating their activity and achieving specificity of their effects in cells (*12, 13*). MBP has been classified as an intrinsically disordered protein (*6*); its unordered structure confers upon it the flexibility to interact with an array of negatively charged surfaces and ligands and to acquire whatever local conformation is necessary to optimize binding to several different targets. In myelin and oligodendrocytes, MBP binds electrostatically to negatively charged lipids such as phosphatidylserine and inositide lipids on the cytosolic surface. Its ability to bind cytoskeletal proteins and signaling proteins containing SH3 domains to a lipid bilayer suggests that it may function as a scaffolding protein in oligodendrocytes or myelin and tether these proteins to the plasma membrane. The interaction of MBP with SH3 domains of proteins, in addition to its already well-established interactions with cytoskeletal proteins, points to a more definite role for MBP in signal transduction. The interaction with Fyn-SH3 is of particular interest because Fyn signaling is involved in regulation of MBP gene expression and participates in the formation of the compact myelin sheath (*53*−*58*).

MBP and Fyn are present together in lipid rafts isolated from myelin (*28, 51, 59*) and shown here to be colocalized in OLs. We have shown further that increasing the negative membrane surface charge by increasing the concentration of PI, or by increasing the number of phosphate groups on PI, i.e., substituting PIP and PIP_2 for PI in the lipid bilayer, weakened the ability of MBP to bind Fyn-SH3 to the membrane surface. Phosphorylation or deimination of MBP also weakened the interaction of Fyn-SH3 with membrane-bound MBP. This could be partly due to conformational

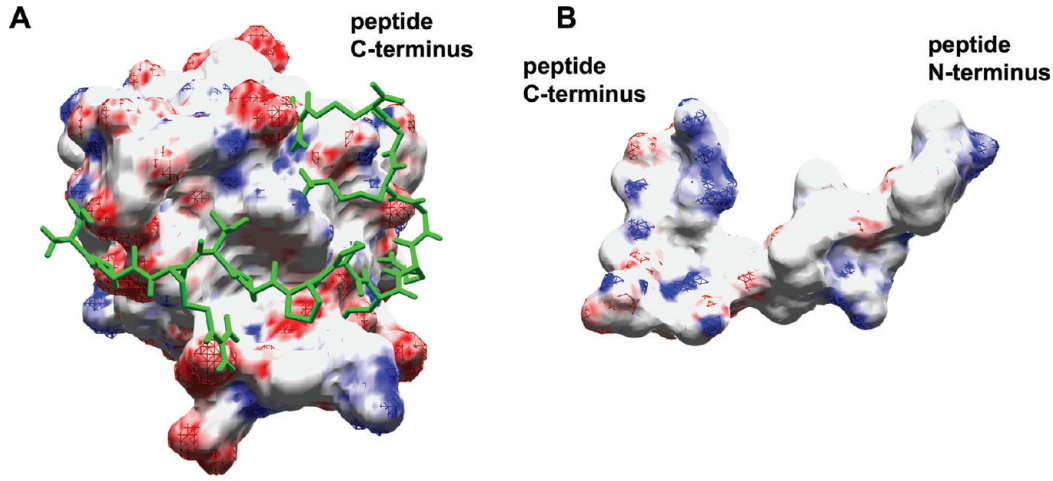

FIGURE 6: Electrostatic potential surfaces of (A) the Fyn-SH3 domain and (B) the MBP T92−R104 peptide, calculated at an ionic strength corresponding to a salt concentration of 100 mM. The cutoff and colors for the surface are as described in the legend of Figure 2. Beneath the electrostatic potential surface, the peptide and the protein domain are represented with their solvent accessible surface, on which the electrostatic potential is mapped. The Fyn-SH3 domain is oriented in the same way as in Figure 2A and the MBP peptide the same way as in Figure 2B. In panel A, the MBP peptide in a green stick representation is superimposed on the Fyn-SH3 domain to show its location, but it is not included in the electrostatic potential calculation.

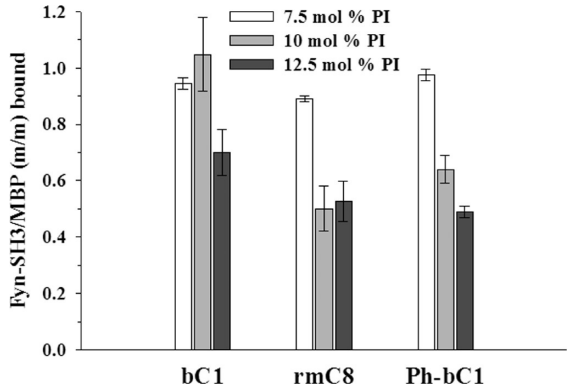

FIGURE 7: Binding of Fyn-SH3 to membrane-associated, post-translationally modifed MBP. The isomers bC1 (unmodified bovine 18.5 kDa MBP), rmC8 (quasi-deiminated recombinant murine 18.5 kDa MBP), and Ph-bC1 (MAPK-phosphorylated bovine C1 isomer) are compared using PC/PI MLV at three different PI concentrations. Amounts of 2.2 nmol of each isomer and of Fyn-SH3 per 500 μg of lipid were used. The plots show the mole ratio of bound Fyn-SH3 to the different membrane-associated MBP isomers at 7.5 mol % PI (white bars), 10 mol % PI (light gray bars), and 12.5 mol % PI (dark gray bars). Data represent the mean ± the standard deviation of three independent experiments.

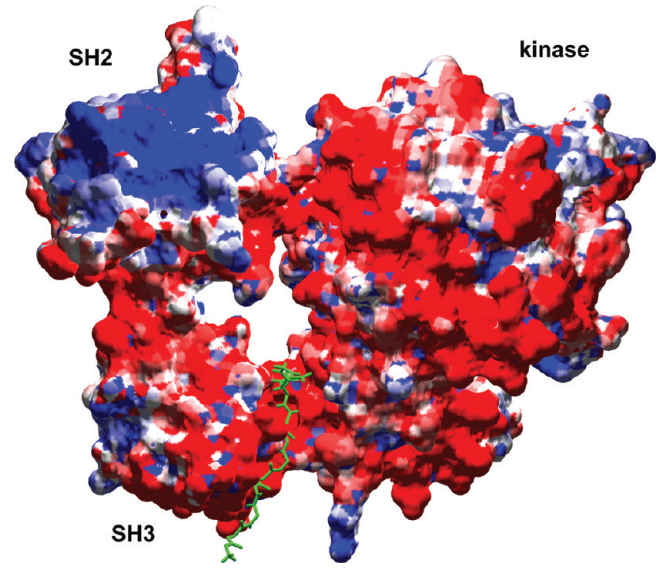

FIGURE 8: Working model of the human Fyn kinase, including the SH2, SH3, and kinase domains, with the MBP T92−R104 peptide complexed to the SH3 domain. The Fyn kinase is represented with its accessible surface colored by electrostatic potential (red for negative and blue for positive). The backbone of the MBP peptide is depicted in green as a stick representation.

changes in MBP. Phosphorylation at some sites has been shown to modify its local conformation and induce some secondary structure (*31, 60, 61*), whereas deimination increased the level of disorder of the protein (*36*). However, modeling of the MBP−Fyn-SH3 complex has shown that phosphorylation of the MBP ligand peptide caused a conformational change in the ligand domain and its side chains but did not predict a significant decrease in the level of binding because new interactions with other Fyn-SH3 residues were able to substitute for those lost (*11*). Phosphorylation and deimination of MBP did not appear to affect its binding in solution to Fyn-SH3 on an array (*11*), although the effect on binding affinity has not yet been measured. Previous studies have shown that the proline-rich region of MBP (the putative SH3 target) is accessible on the bilayer surface for tethering signaling molecules, and its accessibility may be enhanced further by post-translational modifications of MBP that reduce its net positive charge and degree of attachment to the membrane surface, such as deimination, which causes greater exposure of an immunodominant epitope and C-terminal residues on the bilayer surface (*30, 62, 63*). Therefore, the most likely cause of weakened interaction of Fyn-SH3 with phosphorylated or deiminated membrane-bound MBP is the increased net negative surface charge of the membrane.

From our observations presented here, it is suggested that changes in membrane negative surface charge due to protein or lipid modifications, which could occur during cell signaling, can regulate the binding of Fyn-SH3 to membrane-associated MBP and thus could regulate the activity of Fyn at the membrane surface. In fact, the entire Fyn structure has additional large regions of negative potential (Figure 8) that could contribute to the electrostatic repulsion between Fyn and the negatively charged membrane surface, when the

negative charge due to acidic lipids exceeds the positive charge contributed by the highly basic protein MBP. Other proteins with basic domains, such as MARCKS, have been shown to have the phosphorylation-dependent potential to regulate cytoskeletal and signaling proteins through PIP_2-dependent mechanisms, by sequestration of PIP_2 (*19*). However, they have not been shown to bind negatively charged proteins to a membrane, nor has it previously been shown to be possible to modulate scaffold protein-mediated tethering of other proteins to a membrane by changes in membrane surface charge. This is a previously unrecognized potential mechanism of regulating binding and compartmentalization of signaling proteins to membrane domains.

ACKNOWLEDGMENT

We are grateful to Dr. Alan Davidson and Mr. Arash Zarrine-Afsar (University of Toronto) for the Fyn-SH3 domain and to Ms. Godha Rangaraj for preparation of bC1 and Ph-bC1.

REFERENCES

1. Boggs, J. M., Ed. (2008) *Myelin Basic Protein*, Nova Science Publishers, Inc., Hauppauge, NY.
2. Boggs, J. M. (2006) Myelin Basic Protein: A multifunctional protein. *Cell. Mol. Life Sci. 63*, 1945–1961.
3. Demel, R. A., London, Y., van Kessel, W. S. M. G., Vossemberg, F. G. A., and van Deenen, L. L. M. (1973) The specific interaction of myelin basic protein with lipids at the air-water interface. *Biochim. Biophys. Acta 311*, 507–519.
4. Smith, R. (1992) The basic-protein of CNS myelin. Its structure and ligand-binding. *J. Neurochem. 59*, 1589–1608.
5. Boggs, J. M., Moscarello, M. A., and Papahadjopoulos, D. (1982) Structural organization of myelin: Role of lipid-protein interactions determined in model systems. In *Lipid-Protein Interactions* (Jost, P., and Griffith, O. H., Eds.) pp 1−51, Vol. 2, Wiley, New York.
6. Harauz, G., Ishiyama, N., Hill, C. M., Bates, I. R., Libich, D. S., and Farès, C. (2004) Myelin basic protein−diverse conformational states of an intrinsically unstructured protein and its roles in myelin assembly and multiple sclerosis. *Micron 35*, 503–542.
7. Boggs, J. M., and Rangaraj, G. (2000) Interaction of lipid-bound myelin basic protein with actin filaments and calmodulin. *Biochemistry 39*, 7799–7806.
8. Hill, C. M. D., Libich, D. S., and Harauz, G. (2005) Assembly of tubulin by classic myelin basic protein isomers and regulation by post-translational modification. *Biochemistry 44*, 16672–16683.
9. Libich, D. S., Hill, C. M. D., Bates, I. R., Hallett, F. R., Armstrong, S., Siemiarczuk, A., and Harauz, G. (2003) Interaction of the 18.5 kDa isoform of myelin basic protein with Ca^{2+}-calmodulin: Effects of deimination assessed by intrinsic Trp fluorescence spectroscopy, dynamic light scattering, and circular dichroism. *Protein Sci. 12*, 1507–1521.
10. Moscarello, M. A. (1997) Myelin basic protein, the 'executive' molecule of the myelin membrane. In *Cell Biology and Pathology of Myelin: Evolving Biological Concepts and Therapeutic Approaches* (Juurlink, B. H. J., Devon, R. M., Doucette, J. R., Nazarali, A. J., Schreyer, D. J., and Verge, V. M. K., Eds.) pp 13−25, Plenum, New York.
11. Polverini, E., Rangaraj, G., Libich, D. S., Boggs, J. M., and Harauz, G. (2008) Binding of the proline-rich segment of myelin basic protein to SH3 domains: Spectroscopic, microarray, and modeling studies of ligand conformation and effects of posttranslational modifications. *Biochemistry 47*, 267–282.
12. Pawson, T., and Scott, J. D. (1997) Signaling through scaffold, anchoring, and adaptor proteins. *Science 278*, 2075–2080.
13. Kholodenko, B. N., Hoek, J. B., and Westerhoff, H. V. (2000) Why cytoplasmic signaling proteins should be recruited to cell membranes. *Trends Cell Biol. 10*, 173–178.
14. Murray, D., Arbuzova, A., Hangyas-Mihalyne, G., Gambhir, A., Ben-Tal, N., Honig, B., and McLaughlin, S. (1999) Electrostatic properties of membranes containing acidic lipids and adsorbed basic peptides: Theory and experiment. *Biophys. J. 77*, 3176–3188.
15. Arbuzova, A., Wang, L., Wang, J., Hangyás-Mihályné, G., Murray, D., Honig, B., and McLaughlin, S. (2000) Membrane binding of peptides containing both basic and aromatic residues. Experimental studies with peptides corresponding to the scaffolding region of caveolin and the effector region of MARCKS. *Biochemistry 39*, 10330–10339.
16. McLaughlin, S., and Aderem, A. (1995) The myristoyl-electrostatic switch: A modulator of reversible protein-membrane interactions. *Trends Biochem. Sci. 20*, 272–276.
17. Ohmori, S., Sakai, N., Shirai, Y., Yamamoto, H., Miyamoto, E., Shimizu, N., and Saito, N. (2000) Importance of protein kinase C targeting for the phosphorylation of its substrate, myristoylated alanine-rich C-kinase substrate. *J. Biol. Chem. 275*, 26449–26457.
18. Musse, A. A., Gao, W., Homchaudhuri, L., Boggs, J. M., and Harauz, G. (2008) Myelin basic protein as a "$PI(4,5)P_2$-modulin": A new biological function for a major central nervous system protein. *Biochemistry 47*, 10372–10382.
19. McLaughlin, S., and Murray, D. (2005) Plasma membrane phosphoinositide organization by protein electrostatics. *Nature 438*, 605–611.
20. Boggs, J. M., Yip, P. M., Rangaraj, G., and Jo, E. (1997) Effect of posttranslational modifications to myelin basic protein on its ability to aggregate acidic lipid vesicles. *Biochemistry 36*, 5065–5071.
21. Wood, D. D., and Moscarello, M. A. (1989) The isolation, characterization, and lipid-aggregating properties of a citrulline containing myelin basic protein. *J. Biol. Chem. 264*, 5121–5127.
22. Kim, J. K., Mastronardi, F. G., Wood, D. D., Lubman, D. M., Zand, R., and Moscarello, M. A. (2003) Multiple sclerosis: An important role for post-translational modifications of myelin basic protein in pathogenesis. *Mol. Cell. Proteomics 2*, 453–462.
23. Harauz, G., and Musse, A. A. (2007) A tale of two citrullines-structural and functional aspects of myelin basic protein deimination in health and disease. *Neurochem. Res. 32*, 251–256.
24. Mastronardi, F. G., and Moscarello, M. A. (2008) Deimination of myelin basic protein by PAD enzymes and their role in multiple sclerosis. In *Myelin Basic Protein* (Boggs, J. M., Ed.) pp 31−50, Nova Science Publishers, Inc., Hauppauge, NY.
25. Mastronardi, F. G., and Moscarello, M. A. (2005) Molecules affecting myelin stability: A novel hypothesis regarding the pathogenesis of multiple sclerosis. *J. Neurosci. Res. 80*, 301–308.
26. Erickson, A. K., Payne, D. M., Martino, P. A., Rossomando, A. J., Shabanowitz, J., Weber, M. J., Hunt, D. F., and Sturgill, T. W. (1990) Identification by mass spectrometry of threonine 97 in bovine myelin basic protein as a specific phosphorylation site for mitogen-activated protein kinase. *J. Biol. Chem. 265*, 19728–19735.
27. Hirschberg, D., Radmark, O., Jornvall, H., and Bergman, T. (2003) Thr94 in bovine myelin basic protein is a second phosphorylation site for 42-kDa mitogen-activated protein kinase (ERK2). *J. Protein Chem. 22*, 177–181.
28. DeBruin, L. S., Haines, J. D., Wellhauser, L. A., Radeva, G., Schonman, V., Bienzle, D., and Harauz, G. (2005) Developmental partitioning of myelin basic protein into membrane microdomains. *J. Neurosci. Res. 80*, 211–225.
29. DeBruin, L. S., and Harauz, G. (2007) White matter rafting-membrane microdomains in myelin. *Neurochem. Res. 32*, 213–228.
30. Musse, A. A., Boggs, J. M., and Harauz, G. (2006) Deimination of membrane-bound myelin basic protein in multiple sclerosis exposes an immunodominant epitope. *Proc. Natl. Acad. Sci. U.S.A. 103*, 4422–4427.
31. Shanshiashvili, L. V., Suknidze, N. Ch., Machaidze, G. G., Mikeladze, D. G., and Ramsden, J. J. (2003) Adhesion and clustering of charge isomers of myelin basic protein at model myelin membranes. *Arch. Biochem. Biophys. 419*, 170–177.
32. Boggs, J. M., Rangaraj, G., Hill, C. M. D., Bates, I. R., Heng, Y. M., and Harauz, G. (2005) Effect of arginine loss in myelin basic protein, as occurs in its deiminated charge isoform, on mediation of actin polymerization and actin binding to a lipid membrane in vitro. *Biochemistry 44*, 3524–3534.
33. Hill, C. M. D., and Harauz, G. (2005) Charge effects modulate actin assembly by classic myelin basic protein isoforms. *Biochem. Biophys. Res. Commun. 329*, 362–369.
34. Boggs, J. M., Rangaraj, G., Gao, W., and Heng, Y. M. (2006) Effect of phosphorylation of myelin basic protein by MAPK on its interactions with actin and actin binding to a lipid membrane *in vitro*. *Biochemistry 45*, 391–401.

35. Chiefetz, S., Moscarello, M. A., and Deber, C. M. (1984) NMR investigation of the charge isomers of bovine myelin basic protein. *Arch. Biochem. Biophys. 233*, 151–160.
36. Bates, I. R., Libich, D. S., Wood, D. D., Moscarello, M. A., and Harauz, G. (2002) An Arg/Lys→Gln mutant of recombinant murine myelin basic protein as a mimic of the deiminated form implicated in multiple sclerosis. *Protein Expression Purif. 25*, 330–341.
37. Maxwell, K. L., and Davidson, A. R. (1998) Mutagenesis of a buried polar interaction in an SH3 domain sequence conservation provides the best prediction of stability effects. *Biochemistry 37*, 16172–16182.
38. Boggs, J. M., Gao, W., and Hirahara, Y. (2008) Signal transduction pathways involved in interaction of galactosylceramide/sulfatide-containing liposomes with cultured oligodendrocytes and requirement for myelin basic protein and glycosphingolipids. *J. Neurosci. Res. 86*, 1448–1458.
39. Gambhir, A., Hangyas-Mihalyne, G., Zaitseva, I., Cafiso, D. S., Wang, J., Murray, D., Pentyala, S. N., Smith, S. O., and McLaughlin, S. (2004) Electrostatic sequestration of PIP_2 on phospholipid membranes by basic/aromatic regions of proteins. *Biophys. J. 86*, 2188–2207.
40. Peterson, G. L. (1977) A simplification of the protein assay method of Lowry et al. which is more generally applicable. *Anal. Biochem. 83*, 346–356.
41. Guex, N., and Peitsch, M. C. (1997) SWISS-MODEL and the Swiss-PdbViewer: An environment for comparative protein modeling. *Electrophoresis 18*, 2714–2723.
42. Van Gunsteren, W., Billeter, S., Eising, A., Hunenberger, P., Kruger, P., Mark, A., Scott, W., and Tironi, I. (1996) *Biomolecular simulation: The GROMOS96 manual and user guide*, Vdf Hochschulverlag, Zurich.
43. Weiner, S. J., Kollman, P. A., Case, D. A., Singh, U. C., Ghio, C., Alagona, G., Profeta, S., Jr., and Weiner, P. (1984) A new force field for molecular mechanical simulation of nucleic acids and proteins. *J. Am. Chem. Soc. 106*, 765–784.
44. Berman, H. M., Westbrook, J., Feng, Z., Gilliland, G., Bhat, T. N., Weissig, H., Shindyalov, I. N., and Bourne, P. E. (2000) The Protein Data Bank. *Nucleic Acids Res. 28*, 235–242.
45. Jelić, D., Mildner, B., Kostrun, S., Nujić, K., Verbanac, D., Culić, O., Antolović, R., and Brandt, W. (2007) Homology modeling of human Fyn kinase structure: Discovery of rosmarinic acid as a new Fyn kinase inhibitor and in silico study of its possible binding modes. *J. Med. Chem. 50*, 1090–1100.
46. Li, S. S. (2005) Specificity and versatility of SH3 and other proline-recognition domains: Structural basis and implications for cellular signal transduction. *Biochem. J. 390*, 641–653.
47. Reynolds, C. H., Garwood, C. J., Wray, S., Price, C., Kellie, S., Perera, T., Zvelebil, M., Yang, A., Sheppard, P. W., Varndell, I. M., Hanger, D. P., and Anderton, B. H. (2008) Phosphorylation regulates tau interactions with Src homolgy 3 domains of phosphatidylinositol-3-kinase, phospholipase Cγ1, Grb2, and Src family kinases. *J. Biol. Chem. 283*, 18177–18186.
48. Maas, T., Eidenmuller, J., and Brandt, R. (2000) Interaction of tau with the neural membrane cortex is regulated by phosphorylation at sites that are modified in paired helical filaments. *J. Biol. Chem. 275*, 15733–15740.
49. Kawarabayashi, T., Shoji, M., Younkin, L. H., Wen-Lang, L., Dickson, D. W., Murakami, T., Matsubara, E., Abe, K., Ashe, K. H., and Younkin, S. G. (2004) Dimeric amyloid β protein rapidly accumulates in lipid rafts followed by apolipoprotein E and phosphorylated tau accumulation in the Tg2576 mouse model of Alzheimer's disease. *J. Neurosci. 24*, 3801–3809.
50. Klein, C., Kramer, E. M., Cardine, A. M., Schraven, B., Brandt, R., and Trotter, J. (2002) Process outgrowth of oligodendrocytes is promoted by interaction of fyn kinase with the cytoskeletal protein tau. *J. Neurosci. 22*, 698–707.
51. Arvanitis, D. N., Min, W., Gong, Y., Meng, Y. M., and Boggs, J. M. (2005) Two types of detergent-insoluble, glycosphingolipid/cholesterol-rich membrane domains in isolated myelin. *J. Neurochem. 94*, 1696–1710.
52. Otte, L., Wiedemann, U., Schlegel, B., Pires, J. R., Beyermann, M., Schmieder, P., Krause, G., Volkmer-Engert, R., Schneider-Mergener, J., and Oschkinat, H. (2003) WW domain sequence activity relationships identified using ligand recognition propensities of 42 WW domains. *Protein Sci. 12*, 491–500.
53. Umemori, H., Sato, S., Yagi, T., Aizawa, S., and Yamamoto, T. (1994) Initial events of myelination involve Fyn tyrosine kinase signalling. *Nature 367*, 572–576.
54. Umemori, H., Kadowaki, Y., Hirosawa, K., Yoshida, Y., Hironaka, K., Okano, H., and Yamamoto, T. (1999) Stimulation of myelin basic protein gene transcription by Fyn tyrosine kinase for myelination. *J. Neurosci. 19*, 1393–1397.
55. Osterhout, D. J., Wolven, A., Wolf, R. M., Resh, M. D., and Chao, M. V. (1999) Morphological differentiation of oligodendrocyes requires activation of Fyn tyrosine kinase. *J. Cell Biol. 145*, 1209–1218.
56. Seiwa, C., Sugiyama, I., Yagi, T., Iguchi, T., and Asou, H. (2000) Fyn tyrosine kinase participates in the compact myelin sheath formation in the central nervous system. *Neurosci. Res. 37*, 21–31.
57. Sperber, B. R., Boyle-Walsh, E. A., Engleka, M. J., Gadue, P., Peterson, A. C., Stein, P. L., Scherer, S. S., and McMorris, F. A. (2001) A unique role for Fyn in CNS myelination. *J. Neurosci. 21*, 2039–2047.
58. Seiwa, C., Yamamoto, M., Tanaka, K., Fukutake, M., Ueki, T., Takeda, S., Sakai, R., Ishige, A., Watanabe, K., Akita, M., Yagi, T., Tanaka, K., and Asou, H. (2007) Restoration of FcRγ/Fyn signaling repairs central nervous system demyelination. *J. Neurosci. Res. 85*, 954–966.
59. Krämer, E. M., Klein, C., Koch, T., Boytinck, M., and Trotter, J. (1999) Compartmentation of fyn kinase with glycosylphosphatidylinositol-anchored molecules in oligodendrocytes facilitates kinase activation during myelination. *J. Biol. Chem. 274*, 29042–29049.
60. Ramwani, J. J., Epand, R. M., and Moscarello, M. A. (1989) Secondary structure of charge isomers of myelin basic protein before and after phosphorylation. *Biochemistry 28*, 6538–6543.
61. Deibler, G. E., Stone, A. L., and Kies, M. W. (1990) Role of phosphorylation in conformational adaptability of bovine myelin basic protein. *Proteins: Struct., Funct., Genet. 7*, 32–40.
62. Bates, I. R., Boggs, J. M., Feix, J. B., and Harauz, G. (2003) Membrane-anchoring and charge effects in the interaction of myelin basic protein with lipid bilayers studied by site-directed spin labeling. *J. Biol. Chem. 278*, 29041–29047.
63. Bates, I. R., Feix, J. B., Boggs, J. M., and Harauz, G. (2004) An immunodominant epitope of myelin basic protein is an amphipathic α-helix. *J. Biol. Chem. 279*, 5757–5764.

BI8022587